Polish J. Chem., **77**, 591–600 (2003) **PHYSICAL CHEMISTRY**

The Effect of Different Synthesis Procedures on the Texture Properties of MCM-41 Molecular Sieves Modified with Cesium

by I. Nowak[1], A. Michalska[1], M. Ziolek[1*] and W. Wieczorek[2]

[1]*A. Mickiewicz University, Faculty of Chemistry, Grunwaldzka 6, PL-60-780 Poznan, Poland*
[2]*A. Mickiewicz University, Faculty of Biology, Grunwaldzka 6, PL-60-780 Poznan, Poland*

(Received December 30th, 2002; revised manuscript February 3rd, 2003)

The effect of MCM-41 modification by impregnation with cesium salt on the mesoporous structure has been studied by XRD, N_2 adsorption/desorption, electron microscopy (TEM, SEM) and FT infrared spectroscopy in the skeletal region. The MCM-41 sample prepared at room temperature is more fragile to the modification and hydrothermal treatment than the siliceous material obtained by hydrothermal method.

Key words: MCM-41 stability, modification with cesium

There is considerable interest in the development of heterogeneous base catalysts, due to their application, among others, in fine chemicals production. It is well known that alkaline earth metal oxides, especially cesium oxide, can be used as such catalysts [1]. Current research is directed towards the design of the catalysts with very high surface areas. This can be achieved by introduction of cesium species into the mesoporous molecular sieves, possessing high specific surface area. The main problem with those systems is the stability of the matrix after impregnation with cesium salts. Many host systems have been examined in order to improve the stability of such catalyst.

In respect with the above, Kloestra and van Bekkum [2] showed that cesium-exchanged as well as cesium acetate impregnated MCM-41 materials are active base catalysts. Moreover, Weitkamp and co-workers [3] introduced cesium into MCM-41 sample not only *via* impregnation with cesium acetate but also with cesium hydroxide. The results obtained by these groups as well as by Alvarez *et al*. [4] and Ernst *et al*. [5] show that during the ion-exchange and impregnation/calcination procedure the molecular sieves suffer from a considerable loss in specific surface area, specific pore volume and pore diameter. Recently [6] it has been shown, that cesium impregnation/calcination leads to a higher loss of MCM-41 structure/texture parameters than the ion-exchange modification. However, the Cs-exchanged molecular sieves do not exhibit so high basicity as the impregnated samples.

*M. Ziolek; E-mail: ziolek@amu.edu.pl

Taking into account the above, the aim of this study was the preparation and characterisation of Cs-impregnated MCM-41, prepared by using two different methods leading to various texture parameters of parent MCM-41. First one, applied in 1992 [7,8], was the hydrothermal method, leading to solid with surface area of 1000 $m^2 g^{-1}$, while the second one was published by Schumacher *et al*. [9] and looked as a very simple and promising way for the synthesis of this type of solids with surface area higher than 1400 $m^2 g^{-1}$. The latter type of MCM-41 has not been yet applied for the impregnation with cesium salt and thanks to its very high surface area it could appear as a useful matrix. Therefore, in this work its stability after Cs-impregnation/calcination was compared with that of Cs-impregnated MCM-41 prepared *via* hydrothermal method.

EXPERIMENTAL

Syntheses: Samples of purely siliceous MCM-41 were prepared by hydrothermal method from sodium silicate (27% SiO_2 in 14% NaOH; Aldrich) and cetyltrimethylammonium (CTA) chloride (25-wt.% in water; Aldrich). A quantity of 8.08 g of sodium silicate was added to 50 g of distilled water under stirring. A template/water mixture (83.75 g) was admitted after 10 min. The pH of the formed gel was adjusted to 11 and stirred for about 0.5 h before 20 g of distilled water was added. The gel was loaded into a stoppered PP bottle and heated without stirring at 373 K for 24 h. A mixture was then cooled to room temperature and the pH was again adjusted to 11. This reaction mixture was heated again to 373 K for 24 h. The reaction products were filtered, washed with distilled water, dried in air at 323 K and finally calcined at 823 K for 2h in helium flow and then for 15 h in static conditions in air. The sample is denoted in this paper as MCM-41(H).

Synthesis at room temperature (MCM-41(RT)) was performed in the following way: N-hexadecyltrimethylammonium bromide (2.4 g; ACROS) was dissolved in distilled water (50 g) and ethanol (98-vol.%, 50 cm^3; POLMOS-Poland), and aqueous ammonia (32-wt.%, 15.3 cm^3; POCH-Poland) was added to the surfactant solution. The solution was stirred for 10 min and tetraethoxysilane – TEOS (98 wt.%, 3.4 g; Aldrich) was added. After stirring for 2 h at room temperature the resulting solid was recovered by filtration, washed with distilled water and dried in air at ambient temperature. The template was removed by calcination at 823 K for 8 h.

Modifications: The MCM-41(H) and MCM-41(RT) were modified by impregnation with cesium acetate with the loading of cesium of 5 or 7 wt.%. Then the samples were calcined by three different methods. In method A, the final temperature of the calcination was adjusted to 773 K with a ramp of 3 K min^{-1}, while in method B the samples after impregnation were first dried at 393 K for 1 h with a ramp of 3 K min^{-1} and then calcined at 723 K for 4 h with a ramp of 3 K min^{-1}. In the last method C, the samples after impregnation were first dried at 393 K for 1 h with a ramp of 1 K min^{-1} and then calcined at 773 K for 5 h with a ramp of 1 K min^{-1}. Additionally the parent MCM-41(H) and MCM-41(RT) materials were sprayed with the same amount of water, as used for the impregnation process and calcined with the procedure A of calcination. These samples will be denoted as MCM-41(H)-WA and MCM-41(RT)-WA, respectively.

Analytical techniques: The XRD patterns of the powder materials were recorded by a TUR-40 diffractometer using a Ni-filtered Cu ($K\alpha$) radiation operating at 40 kV and 30 mA. The 2Θ range started from 1.4° and with a step of 0.02°. The hkl indices of materials were calculated based on the Bragg diffraction equation. Micromeritics 2010 was used to measure the nitrogen adsorption/desorption isotherms of the materials. Prior to the measurements, the materials were outgassed at 573 K for 3 hours. The BET specific surface area was calculated using BET equation in the range of relative pressure between 0.05 and 0.25. The BJH method was used to calculate the pore volume and the pore size distribution with the use of the desorption branch of the isotherm. A Bruker FTIR Vector spectrometer was used to detect infrared spectra of the MCM-41 molecular sieves and its related samples. The resolution was selected to be 2 cm^{-1} and the number of scans – 64. The samples were dispersed in KBr pellet with slight grinding for FTIR measurements at room temperature. For TEM measurements the powders were deposited on a grid with a holey carbon film and transferred to JEOL 2000 electron microscope, operating at 80 kV. Scanning electron microscopy was performed using a Philips SEM 515.

RESULTS AND DISCUSSION

The XRD patterns for the calcined parent MCM-41 samples featured four well-resolved reflections, as seen in Fig. 1. From Table 1 one can find that these samples exhibit nanometer sizes of pores (~ 3 nm) and very large surface areas, especially for the sample prepared at RT. Both materials, MCM-41(H) and MCM-41(RT), display hexagonal ordered pores revealed by TEM and presented in Fig. 2A and B, respectively. It is clearly visible that the latter sample shows smaller, but not less arranged pores. From the SEM observations (Fig. 3), one can state that MCM-41(RT) presents very uniform monodispersed spheres with a few micrometer size. In contrast to MCM-41(RT), MCM-41(H) is characterized by a less ordered morphology, variably sized, irregularly shaped particles. Moreover, some irregular solid blocks (some of them roundly shaped) with a larger size can be observed.

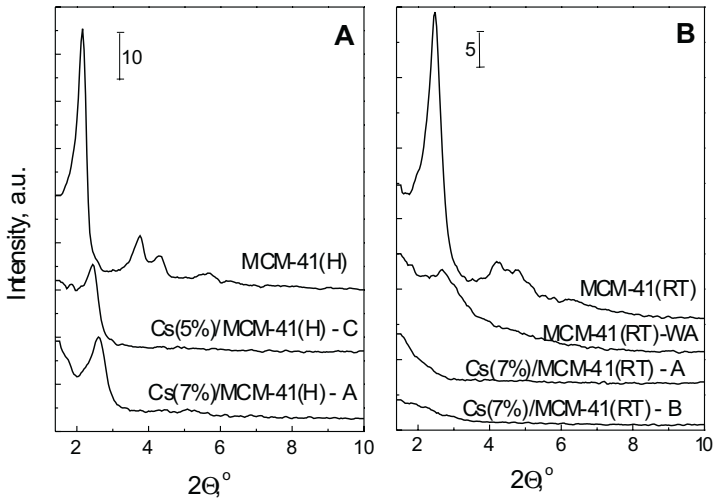

Figure 1. Powder X-ray diffraction patterns of parent and modified MCM-41 samples.

The X-ray diffraction patterns of all modified samples are shown in Fig. 1. Only samples prepared from MCM-41(H) show a distinctive peak at $2\theta = 2–3°$ indexed as [100], while the other peaks are much weaker and overlap each other. Moreover, the peak [100] intensity of these samples decreases after the modification with cesium and is accompanied by a shift towards higher 2Θ (Fig. 1 A). This can suggest a transformation from MCM-41 with the hexagonal structure into a lower-symmetry one [10]. However, the decrease in X-ray peak intensity does not need to be an indication of a partial collapse or a lower regularity of the undimensional arrangement [2]. This can be due to the high electron density of Cs^+ loaded molecular sieves, when using XRD [11]. The presence of the [100] peak indicates that the materials posses ordered long-range structure. Surprisingly, almost no XRD reflection was observed after the impregnation of MCM-41(RT) samples with cesium salt. Moreover, this feature does

not depend on the calcination procedure (Fig. 1B). It seems to be due to a low stability of the matrix, as water introduced during the calcination of MCM(RT) leads to the decrease of the intensity of [100] peak as well. The XRD pattern of the water treated sample, denoted as MCM-41(RT)-WA, is presented in Fig. 1B.

Table 1. Physicochemical data of materials studied.

Sample	d_{100} [I]	BET, [II] $m^2 g^{-1}$	Pore vol., [III] $cm^3 g^{-1}$	Av. pore diam., [III] nm	$R^{IV} = I_{966}/I_{460}$
MCM(RT)	3.562	1179	1.286	3.16	0.251
MCM(RT)-WA	3.296	794	0.247	2.93	0.077
MCM(H)	4.099	988	1.115	3.60	0.170
Cs(7%)/MCM(RT)-A	–	108	0.106	4.70	0.032
Cs(7%)/MCM(RT)-B	–	412	0.220	3.27	0.035
Cs(7%)/MCM(H)-A	3.398	416	0.243	3.91	0.015
Cs(5%)/MCM(H)-C	3.621	591	0.491	3.51	0.011

[(I)] – from XRD; [(II)] – adsorption measurements; [(III)] – calculated by BJH, desorption branch; [(IV)] – from FTIR.

SEM images showed, that after modification by impregnation with cesium salt all the samples reveal the same morphology as both starting materials, *i.e.* Cs(5%)/MCM-41(H)-C and Cs(7%)/MCM-41(H)-A have variably sized, irregularly shaped particles, whereas that of Cs(7%)/MCM-41(RT)-A or -B are very regular.

As it was mentioned above, the ordered structure with hexagonal arrangement of channels of parent materials – MCM-41(RT) and MCM-41(H) – was confirmed by TEM. After impregnation with cesium salt, the MCM-41(H) materials conserve their ordered structure, indicating no effect of modification on the catalyst structure. A well ordered hexagonal array of mesopores (when the electron beam is parallel to their main axis [12]) are observed as seen from Fig. 2 F and G. A very poorly ordered hexagonal structure was observed in the case of MCM-41(RT), used as a matrix for Cs – Fig. 2 D and E. However, a careful examination of the TEM micrographs shows the presence of some topographical features on the surface of round-shaped particles. It seems that the curved cylinders typical of the hexagonal MCM-41 phase are progressively transformed into porous spheres [13]. Some parts of the particles seem to be either thicker than the other parts, or black spots observed on TEM images are the result of pilling several thin particles one above the other, as it was reported by Masson and Pastore [14]. This effect makes difficult a clear observation of the pores. Moreover, one cannot exclude the blockage of the pores by cesium oxide. The sample, made by hydrothermal treatment of the parent MCM-41 material – MCM(RT)-WA – retains the hexagonal arrangement of the pores (Fig. 2C), which was not noticeable by XRD.

Both N_2 adsorption/desorption isotherms of parent materials (Fig. 4) are of type IV in the IUPAC classification and exhibit a sharp inflection at a relative pressure of about 0.35, characteristic of capillary condensation in uniform mesopores. Additio-

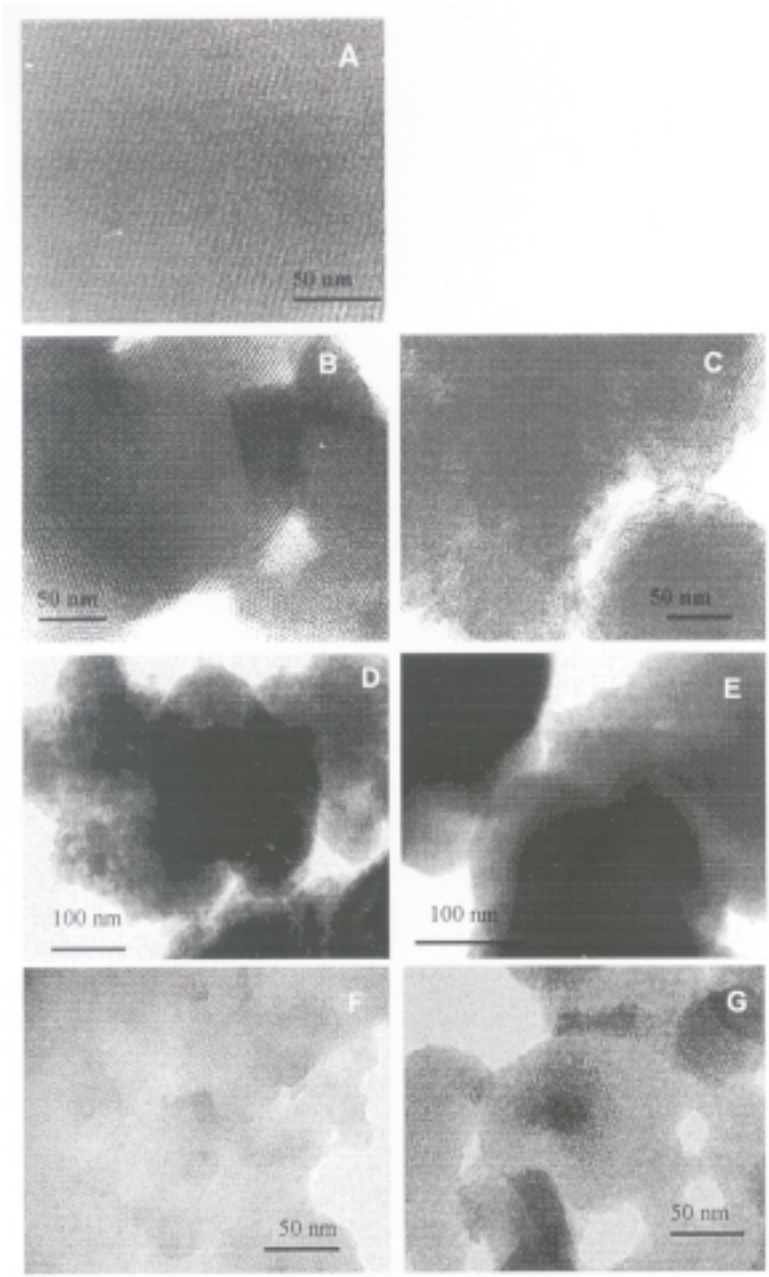

Figure 2. Transmission electron micrographs of: **A** – MCM-41(H); **B** – MCM-41(RT); **C** – MCM-41(RT)-WA; **D** – Cs(7%)/MCM-41(RT)-A; **E** – Cs(7%)/MCM-41(RT)-B; **F** – Cs(7%)/MCM-41(H)-A; **G** – Cs(5%)/MCM-41(H)-C.

nally, almost no hysteresis loop was detected in this region. It is worthy of note, that for both samples (especially that prepared at room temperature) one can observe a very high nitrogen adsorption in mesoporous region (plateau at ~700 cm^3 g^{-1} for

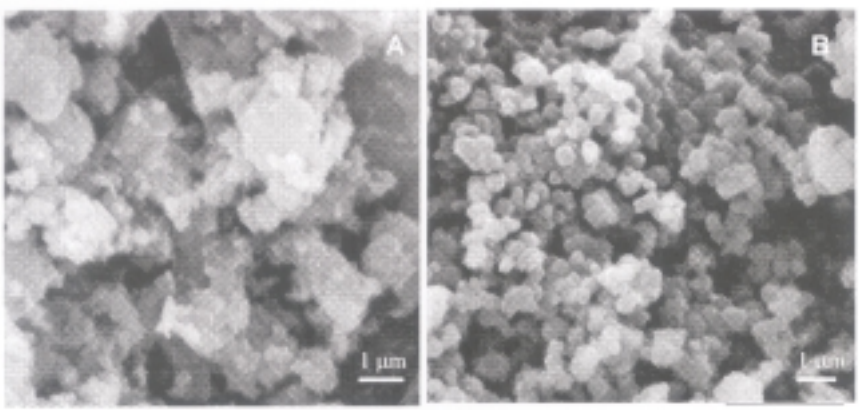

Figure 3. Scanning electron micrographs of: **A** – MCM-41(H) and **B** – MCM-41(RT).

MCM41(RT) and 500 $cm^3 g^{-1}$ – MCM-41(H)). The change of the isotherm shape after the modification by impregnation indicates the degradation of the material, already shown from XRD studies. The pore volume and relative pressure of the inflection decrease after the modification. However, these effects are less evident in the case of the impregnation of MCM-41(H) (see Table 1 and Fig. 4). The reduced pore volumes can be a result of the formation of non-ordered regions in the solid and/or a pore partial narrowing, due to the deposits in the undimensional channels. The accessible pore volume reduction was observed by Ernst *et al*. [4] after the modification with cesium acetate and calcination at 813 K.

The BJH pore distribution indicates a very narrow and monomodal pore size distribution (PSD), centred at around 3 nm for MCM-41(H) and slightly wider – for

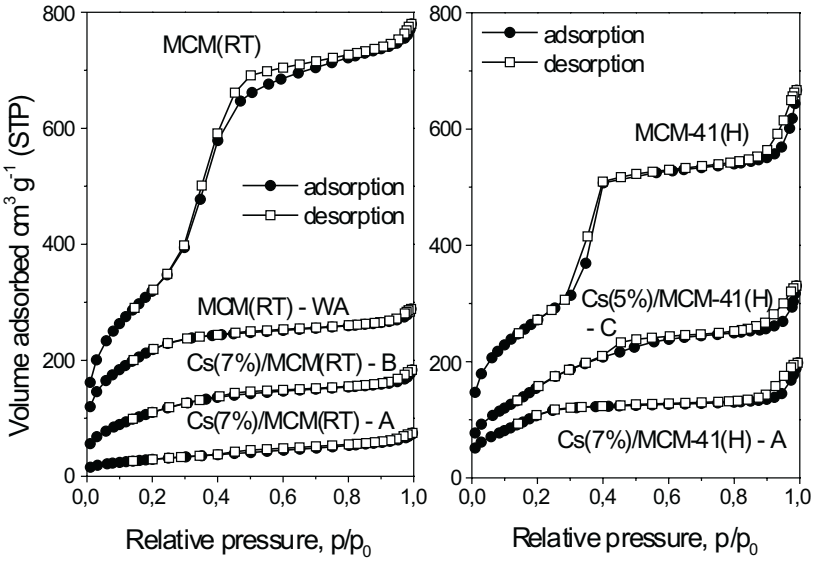

Figure 4. Nitrogen adsorption/desorption isotherms of MCM-41 samples at 77.4 K.

MCM-41(RT) (with the main peak at 2.9 nm – Fig. 5). After the modification with Cs, the mesopores are completely diminished in the case of matrix prepared at RT and are significantly affected for samples obtained by hydrothermal method. There was no macroporosity observed in all samples studied. The systematic decrease of the mesopore volume indicates that the hexagonal pore structure disintegrated readily during the modification process. Moreover, the increase of the baseline in the initial region of the pore size distribution can suggest, being due to the micropore effect, derived from the collapses of the silica wall. As one can see from Table 1, the average pore diameter after modification increases, as well as the pore diameter calculated from the pore size distribution (excepting the material calcined at the highest temperature – 773 K – the sample denoted (C)). Thus, the deposition of the guest component inside the pores and a partial filling have to be excluded. Furthermore, the consideration of interplanar spacing and pore volume suggests a higher wall thickness of materials, prepared *via* hydrothermal method, than that of samples synthesised at RT. This can be the reason of higher stability of MCM(H). It is interesting to add that other authors [24] observed the reduction of the above parameter after modification of MCM-41 material with cesium. Moreover, the instability of MCM-41 after impregnation with cesium species and calcination was investigated by Gabelica and co-workers [15]. The authors showed that this type of modification, as applied in our study, caused a complete damage of the structure, as no peaks were registered on PSD.

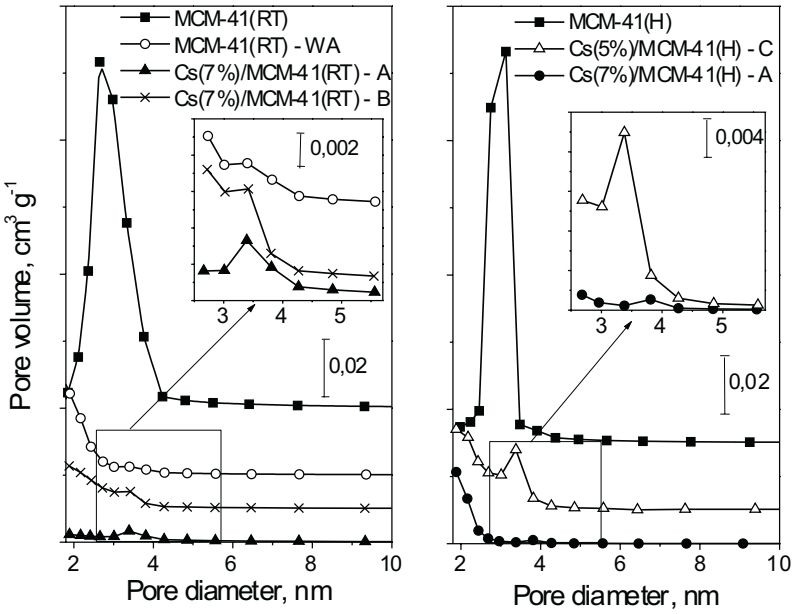

Figure 5. Pore size distribution calculated from the desorption branch of N_2 isotherm of MCM-41 type materials.

The surface area decreases not only after the modification with cesium, but also due to the hydrothermal treatment during the calcination after impregnation. The analysis of data in Table 1 provides a more quantitative indication of the structural damage, that occurs during the modification with cesium acetate and hydrothermal treatment. If one compares the samples with the same loading of cesium, *i.e.* Cs(7%)/MCM-41(RT)-A and Cs(7%)/MCM-41(H)-A, the modification indicates a lower effect, when MCM-41(H) is used as a support. In the case of the first sample, the pore volume decreases to 8% of the initial value, registered for unmodified sample and to 22% for the latter one. Moreover, the surface area decreases to 42% for Cs(7%)/MCM-41(H)-A and dramatically decreases for Cs(7%)/MCM-41(RT)-A to 9% of the value before modification. This again is an evidence for the lack of stability of the sample, made on the matrix synthesized at room temperature. In addition, the hydrothermal treatment of MCM-41(RT) causes the decrease of pore volume to 19% and surface area to 67%. It suggests, that not only the hydrothermal treatment after the impregnation, but also the cation introduced during modification play a role for the loss in structure. Bal *et al.* [16] observed a 50% decrease of the surface area after the modification with cesium at the concentration of 2.25wt.%. In our case, the double amount of Cs introduced to MCM-41(H) caused the same effect.

The FTIR spectra of all samples reveal, besides the bands of well-known vibrational modes of fused silica, an additional band at around 966 cm^{-1}, which one can consider to be related solely with the mesoporous structure of the molecular sieve [17]. This band is associated with the Si–O stretching vibration of a surface hydroxyl group, bonded to a silicon atom [18]. Figure 6 clearly shows that the high surface area and

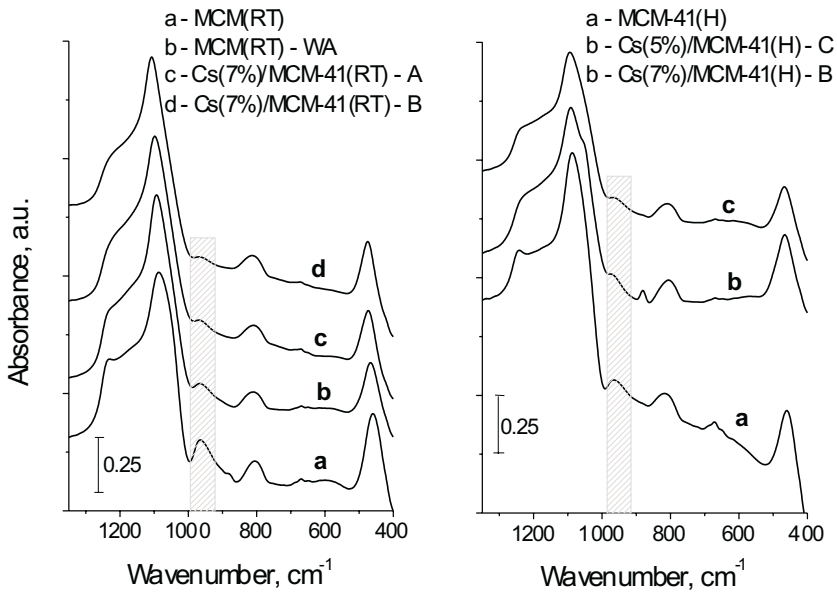

Figure 6. Infrared spectra of MCM-41 samples in the skeletal region.

pore volume of MCM-41(RT) cause a well detection of the surface mode at 966 cm^{-1}. The ratio (R) between the absorbance of a band, which could be assigned to the $Si–O^{\delta-}\cdots H^{\delta+}$ bond (966 cm^{-1}) and a silica structure band (480 cm^{-1}) should give information about the amorphous state – a lower value of R characterizes a more amorphous sample. Table 1 indicates, that this ratio is higher for the sample prepared at RT than that of synthesized by the hydrothermal method. It is accompanied by a higher surface area and pore volume for the first sample. The postsynthesis treatment – impregnation with Cs-acetate or hydrothermal treatment – led to the decrease of the intensity of the band at 966 cm^{-1} and consequently – the R ratio. The partial collapse of ordered mesoporous structure is confirmed by low angle XRD measurements (Fig. 1), while XRD measurements at high angles (Fig. 7) display the amorphous state for modified samples (a broad peaks at *ca*. $2\Theta = \sim 12$ and ~22°). The new amorphous phase can be located inside and/or between mesopores changing the texture and structure of the modified samples.

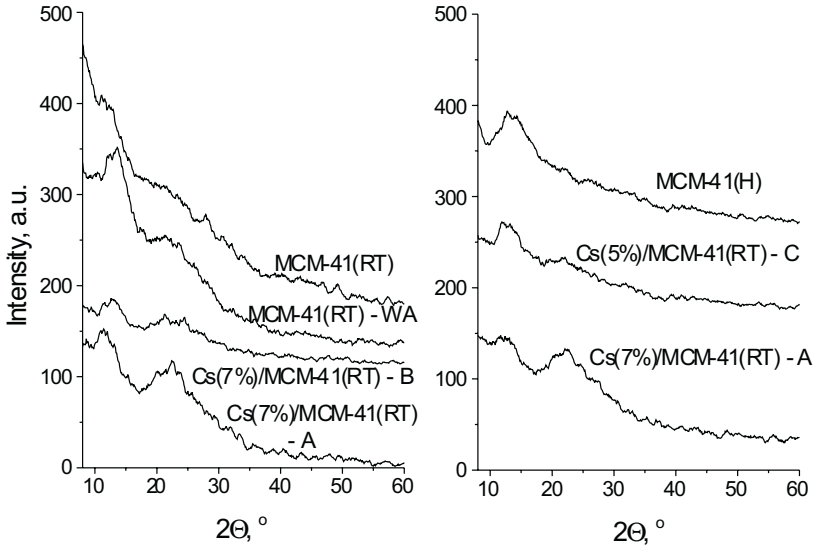

Figure 7. XRD diffractograms at the high angle range.

CONCLUSIONS

The hexagonal arranged structure of both mesoporous siliceous molecular sieves, MCM-41(H) and MCM-41(RT), is partially destroyed (in various range) by the wetness modification with cesium acetate, as well as by the hydrothermal treatment. The destruction is higher, when MCM-41 synthesized at RT is used. Almost completely degradation of this material occurs, due to the impregnation with cesium acetate and hydrothermal treatment. Thus, a very promising method of synthesis (quick and sim-

ple procedure) led to a solid with a very good morphology and structural properties (very high surface area), however, not resistant to the wetness modification and hydrotreatment.

Acknowledgment

This work was supported by the Polish State Committee for Scientific Research, Grant No. 3T09A 102 19.

REFERENCES

1. Barthomeuf, D., *Catal. Rev.-Sci. & Eng.*, **38**, 521 (1996).
2. Kloestra K.R., Van Laren M. and van Bekkum H., *J. Chem. Soc., Farad. Trans.*, **93**, 1211 (1997).
3. Rymsa U., Hunger M., Knözinger H. and Weitkamp J., *Stud. Surf. Sci. Catal.*, **125**, 197 (1999).
4. Alvarez A.M., Bengoa J.F., Cagnoli M.V., Gallegos N.G., Yeramian A.A. and Marchetti S.G., *Stud. Surf. Sci. Catal.*, **142**, 1339 (2002).
5. Ernst S., Bongers T., Casel C. and Munsch S., *Stud. Surf. Sci. Catal.*, **125**, 367 (1999).
6. Ziolek M., Michalska A., Kujawa J. and Lewandowska A., *Stud. Surf. Sci. Catal.*, **141**, 411 (2002).
7. Beck J.S., Vartuli J.C., Roth W.J., Leonowicz M.E., Kresge C.T., Schmitt K.D., Chu C.T.-W., Olson D.H., Sheppard E.W., McCullen S.B., Higgins J.B. and Schlenker J.L*., J. Am. Chem. Soc.*, **114**, 10834 (1992).
8. Schmidt R., Hansen E.W., Stöcker M., Akporiaye D. and Ellestad O.H., *J. Am. Chem. Soc.*, **117**, 4049 (1995).
9. Schumacher K., Grün M. and Unger K.K., *Micropor. Mesopor. Mater.*, **27**, 201 (1999).
10. Zhao D., Huo Q., Feng J., Kim J., Han Y. and Stucky G.D., *Chem. Mater.*, **11**, 2668 (1999).
11. Hathaway P.E. and Davis M.E., *J. Catal.*, **116**, 263 (1989).
12. Bennadja Y., Beaunier P., Margolese D. and Davidson A., *Micropor. Mesopor. Mater.*, **44–45**, 147 (2001).
13. Oberhageman U., Kinski I., Dierdof I., Marler B. and Gies H., *J. Non-Crystalline Solids*, **197**, 145 (1996).
14. Masson N.C. and Pastore H.O., *Micropor. Mesopor. Mater.*, **44–45**, 173 (2001).
15. Noda Pérez C., Moreno E., Henriques C.A., Valange S., Gabelica Z. and Monteiro J.L.F., *Micropor. Mesopor. Mater.*, **41**, 137 (2000).
16. Bal R., Chaudhari K. and Sivasanker S., *Catal. Lett.*, **70**, 75 (2000).
17. Gu G., Ong P.P. and Chu C., *J. Phys. Chem. Solids*, **60**, 943 (1999).
18. Laughlin R.B., Joannopoulos J.D., Murray C.A., Hartnett K.J. and Greytak T.J., *Phys. Rev. Lett.*, **40**, 461 (1978).